Paper 187

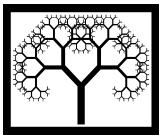


Proceedings of the Eleventh International Conference
on Computational Structures Technology,
B.H.V. Topping, (Editor),
Civil-Comp Press, Stirlingshire, Scotland

# Efficient Linear and Non-Linear Finite Element Formulation using a New Local Enhancement of Displacement Fields for Triangular Elements

**L. Damkilde and R.R. Pedersen**
**Department of Civil Engineering**
**Aalborg University, Esbjerg, Denmark**

## Abstract

This paper describes a new triangular plane element which can be considered as a linear strain triangular element (LST) extended with incompatible displacement modes. The extended element will have a full cubic interpolation of strains and stresses. The extended LST-element is connected with other elements similar to the LST-element *i.e.* through three corner nodes and three mid-side nodes. The incompatible modes are associated with two displacement gradients at each mid-side node and displacements in the central node. The element passes the patch test and converges to the exact solution.

The element has been tested on a standard linear test such as Cook's panel, and is shown as expected to be somewhat more flexible than the LST-element and the compatible quadratic strain element (QST). The extended element has also been applied to material non-linear geotechnical problems. Geotechnical problems often show a very slow convergence, and the numerical solutions will in general overestimate the bearing capacity and underestimate the displacements. The examples show that the extended incompatible element behaves much better than the corresponding compatible elements especially for coarse meshes.

**Keywords:** incompatible element, material non-linear problems, geotechnics.

# 1 Introduction

In geotechnical problems it is often seen that the convergence rate is very low, and that the number of elements has to be rather large in order to obtain an acceptable accuracy for engineering use. In [1], [5] and [6] some examples on slow convergence are given, and the literature can provide many others. In the paper a new type of element is proposed, and the implementation show that the convergence rate is faster.

The proposed element is plane but the principle behind the formulation can also be extended to solid elements.

Finite elements are often formulated based on compatible displacement fields. For plane triangular elements this leads to a series of elements based on linear, quadratic or cubic variation of the in-plane displacements. The displacement fields become complete polynomial fields and the inter-element boundaries are fully compatible. The quadratic elements are considered robust and efficient. However, in e.g. geotechnical calculations with high material non-linearities the convergence rate is rather slow. The convergence problems are often associated with very complex strain and stress variations around singularities typical at corners in the intersection between foundation and soil. Another source for convergence problems is related to the collapse form. In analytical solutions based on perfect plasticity the collapse form is described with different slipline systems. The different soil parts slide along the sliplines, and catching these slipline systems in a numerical model is quite demanding.

Enforcing strict inter-element compatibility demands can in some elements such as a 4 noded plane isoparametric element destroy the convergence rate considerably. This element denoted Q4 as in [2] will have a full linear polynomial interpolation of the displacement but only 1 term to describe the quadratic variations. These so-called incomplete polynomial interpolations will result in a strain interpolation where the only linear polynomial term is associated with the shear strain. This is in contradiction with the physical behaviour and e.g. pure bending in a rectangular element will result in a shear strain. The numerical results will be all too stiff, and this is normally denoted shear loacking. The shear locking can be avoided in different ways. One way is to reduce the order of integration, and in this way the differences in strain interpolation are avoided. Another more elegant and efficient method is to introduce local incompatible displacement fields which results in complete polynomial displacements fields. The local degrees of freedom are eliminated on element level and therefore the computational costs are only marginal increased. The local incompatibilities fulfill the so-called patch test, and therefore the numerical results will converge to the exact solution for fine finite element meshes.

The idea in the paper is to add some incompatible deformation modes in order to improve the convergence rate. In the enhancement of the element it is important to keep the displacement interpolation as complete polynomials in order to avoid locking phenomenon similar to the shear locking. In the present paper the well-known LinearSTrain (LST) element is locally enhanced resulting in a complete cubic displacement field interpolation. The extra degrees of freedom are eliminated locally and thereby the computational costs are not increased significantly. The shape functions are based on the authors previous work [3] on compatible or nearly compatible shear flexible plate elements.

In the following the interpolation of the elements displacement are given together with a short describtion of the numerical implementation. The proposed element is tested on the well-known Cook's panel treated by a number of authors. In the implementation of the material non-linear formulation different approaches are discussed.

The non-linear material implementation is compared to a similar compatible formulation. The convergence rate in a typical geotechnical problem shows that the proposed element gives a considerably improvement.

# 2 Extended LST-element

The interpolation functions are expressed in area coordinates, and $\lambda_i, \quad i = 1, 2, 3$ defines a point in the triangle. The sum of the three area coordinates $\lambda_i$ is 1, and $\lambda_i$ is the fraction of the area of the element area that the triangle given by the point and the side opposite to corner node $i$ defines. For more details readers are referred to [2].

## 2.1 Interpolation of in-plane displacements $u$ and $v$

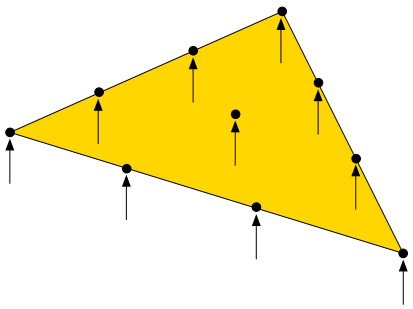

Figure 1: Degrees of freedom v

The starting point is a cubic interpolation of $u$ and $v$, and this will lead to 10 parameters for each displacement. A straight forward way is to interpolate $u$ and $v$ from the horisontal and vertical displacements in the 10 nodes shown in Figure 1. The shape functions can be constructed directly through simple geometrically considerations. For the corner nodes the interpolation function is proportional to a product of 3 lines parallel with the opposite side and each passing through 2, 3 and 4 nodes respectively. For the mid-side nodes a similar approach can be used choosing first a line along the nearest side, a line parallel to the farthest side through the other mid-side node and a line along farthest side. The central node is constructed by the lines along the sides of the triangle. The scaling of the interpolation functions is done by setting the function to 1 for the interpolated nodal position.

However it shows to be more suitable to have the 2 midside displacements converted into a displacement and a displacement gradient in the midpoint of the side as shown in Figure 2. The shape functions are a little more complicated, but can be constructed via the shape functions from the configuration shown in Figure 1.

The shape functions for the in-plane displacement $u$ and $v$ are defined by:

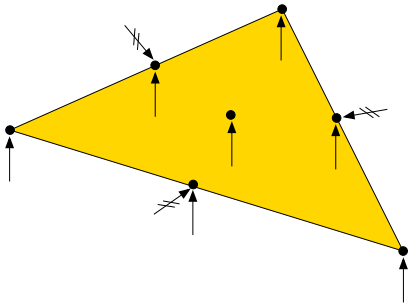

Figure 2: Degrees of freedom v

$$N_i = \lambda_i \left(2\ {\lambda_i}^2 + 2\ {\lambda_j}^2 + 2\ {\lambda_k}^2 + 3\ \lambda_j \lambda_k - 1\right) \qquad i = 1, 2, 3 \tag{1}$$

where $i, j, k$ is a cyclic permutation of the nodal numbers $1, 2, 3$.

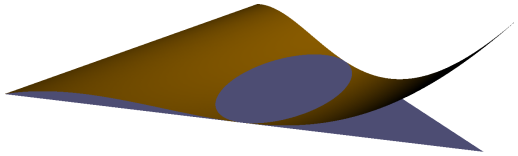

Figure 3: Shape function for displacment in corner node

The shape function is defined by the product of a line defined by the opposite side ($\lambda_i = 0$) and an ellipsis. The ellipsis passes through the center node and the two midside nodes adjacent to the corner node in question. Furthermore the two sides related to the corner node are tangents to the ellipsis. This is illustrated in Figure 3 where the in-plane displacement for clarity is depicted perpendicular to the plane. The part of the shape function that is negative has been removed in order to illustrate the ellipsis.

The shape functions for the displacement in the midside node are given by:

$$N_{3+2i-1} = 12\ \lambda_i\ \lambda_j\ (-\lambda_k + \frac{1}{3}) \qquad i = 1, 2, 3 \tag{2}$$

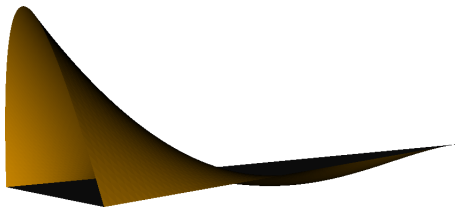

Figure 4: Shape function for displacement in midside node

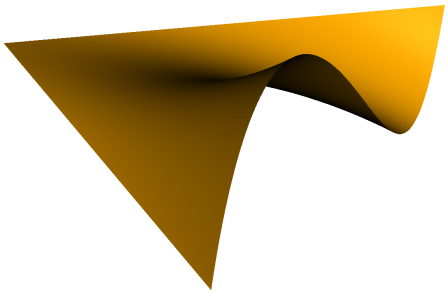

Figure 5: Shape function for displacement gradient in midside node

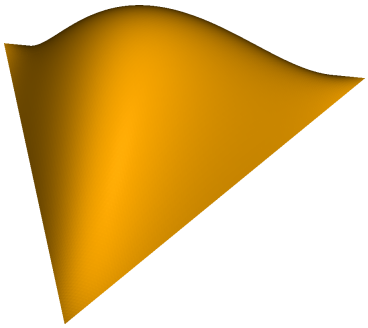

Figure 6: Shape function for center node

The shape function is defined by the product of 3 lines. Two of the lines are the lines defining the other two sides, and the last line is defined by a line going through the center node and parallel to the midside in question. The shape function is illustrated in Figure 4.

The shape functions for the displacement gradient in the midside node are given by:

$$N_{3+2i} = \ell_k \; 2 \; \lambda_i \; \lambda_j \; (\lambda_i - \lambda_j) \qquad i = 1, 2, 3 \tag{3}$$

where $\ell_k$ is the length of the side opposite to node $k$.

The shape function is defined by the product of 3 lines. Two of the lines are the lines defining the other two sides, and the last line is defined by a line going through the midside node and the opposite corner node. The shape function is illustrated in Figure 5.

The shape function for the center node is given by the bubble function, and it is illustrated in Figure 6. :

$$N_{10} = 27 \; \lambda_1 \; \lambda_2 \; \lambda_3 \tag{4}$$

## 2.2 Incompatible displacement gradients

The suggested displacement interpolation based on nodal displacements and displacement gradients will be equivalent to a displacement interpolation based purely on displacements as shown in Figure 1. However the displacement interpolation based on displacements and displacement gradients makes it possible to introduce minor incompatibilities which according to the patch test is legal. In the present approach we do not enforce continuity in displacement gradients across element boundaries. The interelement incompatibility may result in a inter-element sliding along the element side and a difference in displacements perpendicular to the element side. The incompatibilty will fulfill the patch test as the incompatibility error is cancelled at element side. This can most easily be seen from the displacement perpendicular to the side. The displacement gradient will result in a S-shaped formed displacement along the element side. The displacement is 0 in the corners and in the middle and in average there will be no incompatibility.

## 2.3 Finite Element implementation

The Finite Element implementation is straight forward and only a few subjects will be high-ligthed. The stiffness matrix will be calculated numerically by means of Gauss integration in area coordinates. The strains/stresses will be quadratic polynomials, and this enforces 6 Gauss points in order to have an exact integration. The consistent load vector for either surface or volume load may have a component in the displacement gradients, and this has to be taken into account. The procedure depends on the elimination procedure for the displacement gradients.

The incompatible displacement gradients can be handled in two ways. The 6 displacement gradients and the 2 displacements in the central node can be eliminated on element level reducing the number of degrees of freedom to a LST element. If this is done local loads on the eliminated nodes should be transferred properly to the remaining nodes. The method is standard and can e.g. be found in [2]. In the postprocessing the displacements in the eliminated nodes should be calculated again taking into account the local load. The strain/stress calculation can then be done based on a full cubic displacement interpolation.

If the 8 degrees of freedom are not eliminated at element level the number of degrees of freedom will be considerably larger. The advantage is a simpler implementation of the postprocessing. Furthermore an implementation with all degrees of freedom would easily enable both a compatible and incompatible formulation. In the case of a compatible formulation which is identical to an QST-element the direction of the displacement gradients would differ between two adjecent elements, and a general procedure for choosing the direction in the total formulation should be given.

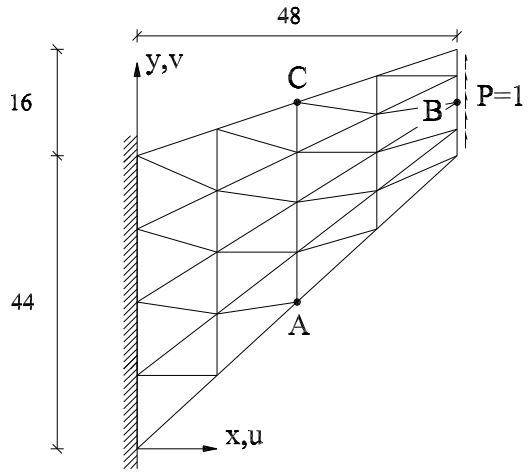


Figure 7: Example

# 3 Linear test - Cook's panel

The proposed element has been tested on different examples. The simple stress states such as constant and linear varying stresses can be reproduced without any error. In more complex examples the convergence of the element has been tested. As expected the displacements converged from above, and in the limit the results will converge to the same values as e.g. the Linear Strain Triangle or with the Quadratic Strain Triangle.

In Figure 7 the well-known Cook's panel is shown. This example has been used as benchmark for test of new plate/membrane elements. In [4] Felippa and Alexander have presented results for Cook's panel.

In this context we only compare the vertical displacement in B, and the results are given in Table 1. The results are scaled on the value $23.9653$ which according to our calculations are a little more accurate than the value $23.95$ used in [4].

| Mesh | LST | ExtLST |
|---|---|---|
| $2 \times 2$ | 0.9723 | 1.1168 |
| $4 \times 4$ | 0.9955 | 1.0365 |
| $6 \times 6$ | 0.9981 | 1.0167 |
| $8 \times 8$ | 0.9988 | 1.0084 |
| $10 \times 10$ | 0.9990 | 1.0045 |
| $16 \times 16$ | 0.9994 | 1.0008 |
| $32 \times 32$ | 0.9998 | 1.0002 |

Table 1: Vertical displacement $v_B$

The convergence has also been shown in Figure 8. The convergence is not as good

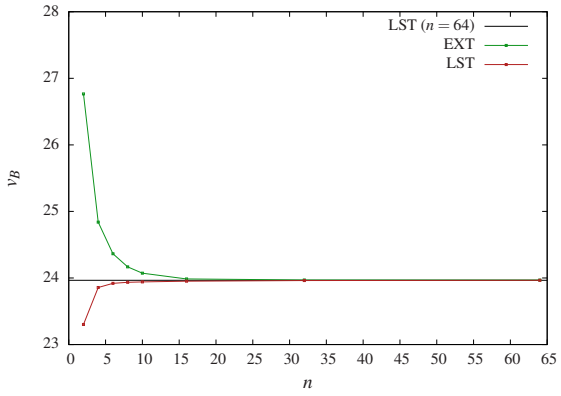


Figure 8: Convergence for Cook's panel - LST and Extended LST element

as the Linear Strain Triangle, but both formulations converge to the same value.

The proposed element is as expected somewhat more flexible than the corresponding compatible formulation of the same element. In linear static cases this is of minor interest, but the incompatible formulation in connection with a compatible formulation can be used to bound the exact energy and displacement values. The potential of the element is expected to be larger in material non-linear problems, where compatible formulation in several cases gives a very slow convergence.

# 4 Formulation of Material non-linear problems

In the solution of the linear static problems the local incompatible deformations can be eliminated a priori. In this respect the Extended LST element can be considered a superelement with 12 external degrees of freedom and 8 internal degrees of freedom. In the postprocessing the internal degrees of freedom can be determined based on the 12 external degrees of freedom, and in the calculation of the strains and stresses the full cubic interpolation of displacements are taken into account. The superelement can be regarded as a cubic displacement interpolation where the reduction from 20 to 12 variables reduces the free parameters in the cubic interpolation. This is equivalent to a static condensation in dynamic problems, see e.g. [2]. In calculation of load and strains/stresses the eliminated variables have to be taken into account as mentioned in a previous section.

In material non-linear problems two different approaches can be used. In the first approach the a priori elimination of 8 degrees of freedom defines a subset of the cubic interpolation defined by the elastic stiffness of the element. This approach will lead to a softer respons than the LST element, but it can not adjust to the gradually reduction in stiffness due to plasticity. The advantage is that the numerical implementation is faster, as the local elimination of variables defining the subset of cubic interpolation is only done 1 time.

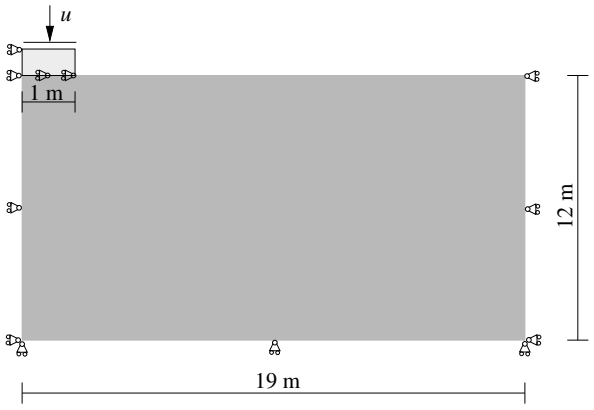


Figure 9: Example: Foundation

The second approach which is used in the paper is to eliminate in every iteration step. This allows for a gradually change in stiffness, and also reduces some of the administrative problems in transferring the residual load from eliminated variables to the remaining 12 variables. The price is an increase in execution time. At present the formulation is working correctly but it is expected that the method can be refined in order to reduce the computing time.

In the current implementation only the Mohr-Coulomb criteria has been implemented, but other non-linear material models can directly be implemented. In the calculation of the consistent plastic material stiffness matrix ($D_p$) and in updating the stresses the methods described in [5] and [6] are used.

# 5 Example

In order to demonstrate the method the bearing capacity of the foundation shown in Figure 9 has been determined.

The material obeys the Mohr-Coulomb criteria and the friction angle is $\phi = 30^o$ and the cohesion is $c = 0$. The plastic model is an associated model i.e. the plastic strains are perpendicular to the yield surface. The coefficient of earth pressure at rest $k_0 = 1$ and the soil weight is taken to be $15$ kPa. The foundation is in this model considered rigid, and the interface between foundation and soil is sufficiently rough to prevent sliding of the soil along the foundation.

The example has been calculated by 2 different element meshes as shown in Figur 10. The coarse mesh on the top is referred to as mesh 1 and the finer mesh as mesh 2. Details in the element mesh around the corner stress singularity can not be seen in the plot, but it is of no importance in this context. We have chosen a structured mesh, but an unstructured would have lead to the same conclusions.

In Figure 11 the load-deflection curve calculated with either LST-elements or Extended LST-elements is shown. The theoretical value is the maximum load calculated

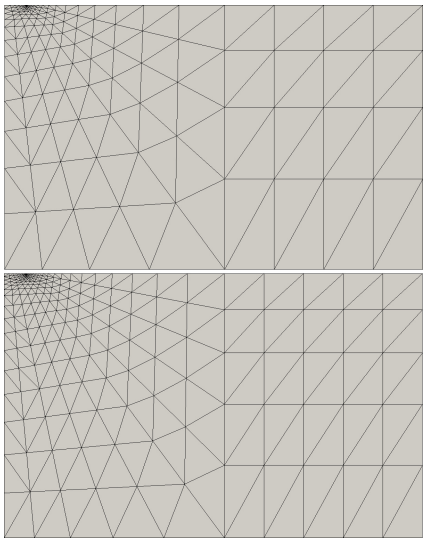

Figure 10: Finite element meshes

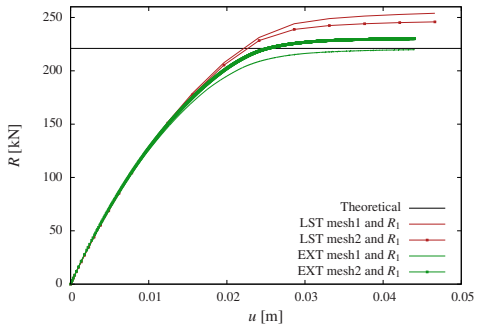


Figure 11: Load-deflection curves for extended LST elements and LST elements

by an upper-bound method for a perfect plastic material model, see [7]. The Figure shows that the extended LST element for both meshes gives a better estimate of the load bearing capacity. A little surprisingly the finest mesh with extended LST elements gives a little overshoot compared to the theoretical value, but it is much more limited than the corresponding results for LST-elements.

In Figure 12 the load-deflections curve calculated with extended LST-elements using different convergence criteria ($R_2$ is the finest). The calculations seem to be somewhat more sensitive to the convergence criteria than similar calculations with the LST element. This phenomena has to be investigated further in order to secure a robust method.

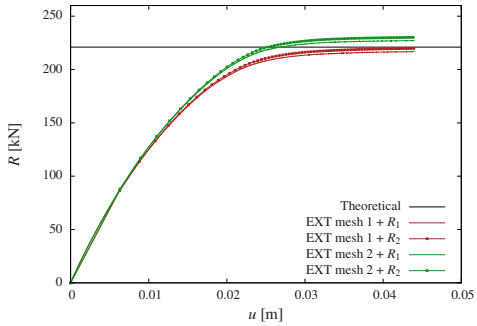


Figure 12: Load-deflection curves for different convergence criteria

# 6 Conclusion

An extended LST element has been formulated, which locally allows a quadratic strain or stress variation, but globally only involves degrees of freedom similar to a LST element. The formulation is based on incompatible displacement modes, which passes the patch test. The extended LST element has been implemented in a finite element system, and linear tests show that the element as expected gives larger displacements (upper-bound) than LST elements (lower bound). The extended LST element has also been used for non-linear material problems. The example shows that the extended LST element gives better results than the LST element for a typical geotechnical problem. The numerical implementation of the extended LST element has to be further refined in order to provide an element as robust as the LST. The extended LST element has the potential to improve the quality and accuracy of geotechnical calculations which generally have a very slow convergence rate.

# References

[1] J. Clausen, L. Damkilde, K. Krabbenhft, ”Efficient Finite Element Calculation of N$\gamma$”, in B.H.V. Topping, (Editor), ”Proceedings of the Eleventh International Conference on Civil, Structural and Environmental Engineering Computing”, Civil-Comp Press, Stirlingshire, UK, Paper 20, 2007. doi:10.4203/ccp.86.20

[2] R.D. Cook, D.S. Malkus, M.E. Plesha and R.J. Witt. *Concepts and Applications of Finite Element Analysis*, Wiley, 4 edition, 2002.

[3] L. Damkilde, R.R. Pedersen, ”A New Accurate yet Simple Shear Flexible Triangular Plate Element with Linear Bending Strains”, in B.H.V. Topping, J.M. Adam, F.J. Pallars, R. Bru, M.L. Romero, (Editors), ”Proceedings of the Tenth International Conference on Computational Structures Technology”, Civil-Comp Press, Stirlingshire, UK, Paper 288, 2010. doi:10.4203/ccp.93.288.

[4] Felippa, C.A. and Alexander, S., “Member triangles with corner drilling freedoms - III Implementation and performance evaluation.“ , Finite Elements in

Analysis and Design, Vol. 12, pp. 203-239, 1992.

[5] Clausen, J., Damkilde, L. and Andersen, L. “An Efficient Return Algorithm for Non-Associated Mohr-Coulomb Plasticity“, Computers & Structures, Vol. 85, pp. 1795-1807, 2007.

[6] Clausen, J, Damkilde, L. and Andersen, L. “Efficient return algorithms for associated plasticity with multiple yield planes“, International Journal for Numerical Methods in Engineering, Vol. 66, Issue 6, pp. 1036-1059, 2006.

[7] Martin, C.M.,“Exact bearing capacity calculation using the methods of characteristics“, In Proceedings of the 11th International Conference of IACMAG, Turin, Italy, 4:441-450, 2005.